Available online at www.sciencedirect.com
ScienceDirect
European Polymer Journal 43 (2007) 1635–1644
EUROPEAN POLYMER JOURNAL
www.elsevier.com/locate/europolj

Macromolecular Nanotechnology

Effect of epoxy resin on rheology of polycarbonate/clay nanocomposites

Defeng Wu, Lanfeng Wu, Ming Zhang *, Liang Wu

School of Chemistry and Chemical Engineering, Yangzhou University, Jiangsu 225002, PR China

Received 6 December 2006; received in revised form 24 January 2007; accepted 4 February 2007
Available online 16 February 2007

Abstract

Polycarbonate/clay nanocomposites (PCNs) were prepared by melt intercalation using epoxy resin as a compatibilizer. The intercalated structure of PCNs was investigated using XRD and TEM. The linear and nonlinear dynamic rheological properties of PCNs were measured by the use of a parallel plate rheometer. The results reveal that the presence of epoxy influences rheological behavior of PCNs significantly. Addition of epoxy can improve dispersion of clay, enhancing the low-frequency viscoelastic responses; while high loadings of epoxy lead to a severe degradation of PC matrix, decreasing the high-frequency responses together with the plasticizing effect of excessive epoxy. Both of these two effects result in invalidity of time–temperature superposition. Moreover, all samples show high sensitivity to both the quiescent and large amplitude oscillatory shear (LAOS) deformation, despite enhanced percolation of tactoids due to the compatibilization of epoxy.

Keywords: Polycarbonate; Clay; Nanocomposites; Rheology; Thermal stability

1. Introduction

Polymer layered silicate nanocomposites (PLSNs) have received much interest over the past decade in research and development as an alternative to conventional filled composites because their unexpected properties, and the potential of becoming a new class of high-performance engineering materials [1–3]. The property enhancement is attributed to the nanometer size and high aspect-ratio characteristics of the individual platelet, and to the well-dispersed, exfoliated nanoclay structure.

Polycarbonate (PC) has outstanding ballistic impact strength and good optical clarity, and is used widely in many transparent engineering applications. The drawbacks of PC include its susceptibility to many organic solvents and poor resistance to abrasion. Thus PC has been modified and tailored in many different ways, particularly by blending with other polymers for use in demanding applications [4]. Recently, the nanocomposite technology has also been applied in the modification of PC, compounding with clay mineral to improve the physical and mechanical properties of PC materials. Hitherto many works have been reported on the

* Corresponding author. Tel.: +86 514 7975590/9115; fax: +86 514 7975244.
E-mail address: dfwu@yzu.edu.cn (M. Zhang).

0014-3057/$ - see front matter © 2007 Elsevier Ltd. All rights reserved.
doi:10.1016/j.eurpolymj.2007.02.013

preparation and characterization of PC/clay and PC alloy/clay nanocomposites (PCNs) [5–17]. The nanoscaled morphology, mechanical properties, thermal stability, and color formation as well as crystallization behavior of PCNs are investigated extensively. On those reported results, it can be concluded that PCNs show significant enhancement in the processing and mechanical properties in contrast to that of neat PC, although addition of clay leads to more or less a decrease of thermal stability of PC matrix.

It is believed that the outstanding properties of PLSNs derive from the unique phase morphology and improved interfacial properties. Recently, rheometry has been proved to be a powerful tool for investigating the internal microstructure and mesoscopic structure of PLSNs because the melt-state rheological characteristics, particularly the low-frequency linear viscoelastic response, of the PLSNs are strongly affected by the mesoscopic structure of the nanoclay [18–29]. Rheological properties of PCNs have also been studied [7,8]. Like other PLSNs, formation of a three-dimensional network structure, due to the anisotropy associated with the nanoclay tactoids, above the percolation threshold leads to an incomplete relaxation or pseudo-solid-like behavior when subjected to small-amplitude shear. However, those studies mainly focus on linear rheological properties. Since the region of linear viscoelastic behavior is very sensitive to the presence of clay, the study on linear viscoelastic properties of PCNs is limited in a quite narrow strain region. Therefore, nonlinear rheological measurements are necessary to facilitate further insight into the internal structure of PCNs.

In our work, at first we used epoxy resin as a compatibilizer to prepare intercalated PCNs by melt mixing. Then, we conducted both the linear and nonlinear rheological measurements on those PCNs. The viscoelastic responses to dynamic and steady shear deformation were detailedly investigated, aiming at exploring how epoxy resin influence on rheological behaviors, further relating viscoelastic responses to the mesoscopic structure of clay tactoids and thermal stability of PCNs.

2. Experimental

2.1. Material preparation

The bisphenol A polycarbonate (PC, 201-10) used in this study is a commercial product of LG-Dow Chemical Co. Ltd., USA. Its MFI is 10 g/10 min (ASTM D1238), and density is 1200 kg/m^3 (ASTM D792). The organoclay (trade name is DK2) was supplied by Fenghong Clay Co. Ltd., PR China, modified with methyl tallow bis(2-hydroxyethyl) ammonium. The epoxy resin used was E51, a bisphenol A diglycidyl ether-based resin made by Shanghai Synthetic Resin Co. Ltd., PR China. Its average molecular weight is about 390 g/mol and the epoxide equivalent weight is about 0.51 g/equiv. PC/clay nanocomposites (PCNs) were prepared by direct melt compounding DK2 and epoxy E51 with PC in a HAAKE Polylab Rheometer (Thermo Electron Co., USA) at 230 °C and 50 rpm for 8 min. The compositions of the PCNs were listed in Table 1. A blank sample, PC/epoxy composite (PCCs), was also prepared using Rheometer for better comparison. All the materials were dried at 80 °C under vacuum for 8 h before using.

Table 1
Compositions and abbreviation of the prepared hybrids

Sample	Comp. (wt%)		
	PC	Clay (DK2)	Epoxy (E51)
PCN2	98	2	0
PCN4	96	4	0
PCN6	94	6	0
PCN22	96	2	2
PCN24	94	2	4
PCN26	92	2	6
PCN42	94	4	2
PCN44	92	4	4
PCN46	90	4	6
PCC4	96	0	4

2.2. Microstructure characterization

The degree of swelling and the interlayer distance of clay in PCNs samples were determined by X-ray diffractometer (XRD). The experiments were performed using a D8 ADVANCE diffractometer (BRUKER AXS Co., Germany) with Cu target and a rotating anode generator operated at 40 kV and 200 mA. The scanning rate was 2°/min from 1° to 10°. The film sample for XRD measurement was prepared by compression molding at 250 °C and 10 MPa. The transmission electron micrographs were taken from 80 to 100 nm thick, microtomed sections using a Tecnai 12 transmission electron microscope (TEM) (PHILIPS Co., Netherlands) with 120 kV accelerating voltage. The morphologies of the fractured surfaces of the samples

were investigated using a PHILIPS XL-30ESEM scanning electron microscope (SEM) with 20 kV accelerating voltage. The sheet samples were kept in liquid nitrogen and then brittle fractured. An SPI sputter coater was used to coat the fractured surfaces with gold for enhanced conductivity.

2.3. Rheological measurements

Rheological measurements were carried out on a rheometer (Haake RS600, Thermo Electron Co., USA) equipped with 20 mm diameter plate. All measurements were performed with a 200 FRTN1 transducer with a lower resolution limit of 0.02 g cm. The samples about 1.0 mm in thickness were melted at 230 °C for 10 min in parallel plate fixture to eliminate residual thermal history, and then carry out experiments immediately. In the dynamic rheological measurements, both the small amplitude oscillatory shear (SAOS) and the large amplitude oscillatory shear (LAOS) were applied. The dynamic strain sweep measurements were carried out firstly to determine the linear region. The dynamic frequency sweep were then carried out on the samples (presheared or not) at the strain of 1% for SAOS measurements, while carried out at the strain of 20%, 50% and 80% for LAOS measurements.

2.4. TGA analyses

All TGA analyses were performed on a Netzsch Instruments STA409PC (Germany). Samples of 10–12 mg were heated from room temperature to 800 °C at the rate of 10 °C/min under nitrogen atmosphere. All TGA results are the average of a minimum of three determinations and the temperatures are reproducible to ±1 °C.

3. Results and discussion

3.1. Microstructure in PCNs

The microstructure and morphology of PLSNs is typically elucidated using XRD and TEM. Fig. 1 shows the XRD patterns of the pristine clay and PCNs. Compared with that of DK2 powder, the diffraction peak of (0 0 1) plane of clay in PCN4 shows a significant shift to lower angles. Basing on Braggs formula, the calculated d_{001} distance expands from 2.10 nm to about 3.26 nm. It indicates that PC chain has crawled into the clay galleries during melt mixing process. With addition of epoxy,

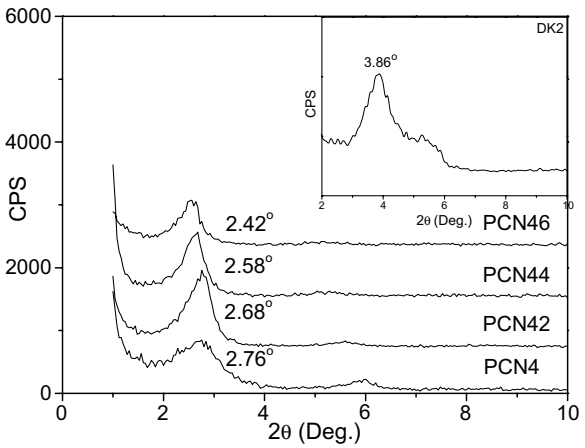

Fig. 1. XRD patterns for clay DK2 and PCNs samples.

the diffraction peak shifts to low angles gradually, and the interlayer space of tactoids increases from 3.26 to 3.80 nm, suggesting that the third component, epoxy, acts as a compatibilizer to facilitate intercalation of PC chain due to its nice affinity to both the PC matrix (analogical bisphenol A structure) and clay (polar interactions) [30]. This effect of assistant intercalation (or co-intercalation) by epoxy has been found in many other PLSNs [25,31–39]. Also, the driving force of this co-intercalation has been widely investigated and is not discussed here again. Note that the existence of sharp Braggs peaks shows that all PCNs samples still retain an intercalated structure after melt-mixing. But the secondary diffraction peak is weakened or even disappears with increasing of epoxy loadings. Therefore, it can be speculated that PCN4 sample may present a well ordered intercalated structure, while addition of epoxy leads to formation of the disordered intercalated structure of clay tactoids.

TEM study was then carried out to further confirm dispersion state of clay in the nanocomposites. Fig. 2a and b give the TEM image of PCN4 and PCN44 samples, respectively. Clay tactoids in PCN4 sample present a typical intercalated structure in ordered stacked. However, with addition of epoxy, those intercalated tactoids show a loose and incompact morphology, as can be seen clearly in Fig. 2b. Accordingly, the observations from TEM are in agreement with the results from XRD.

3.2. Linear dynamic rheological properties

The dynamic strain sweep was firstly conducted to determine linear viscoelastic region of the samples.

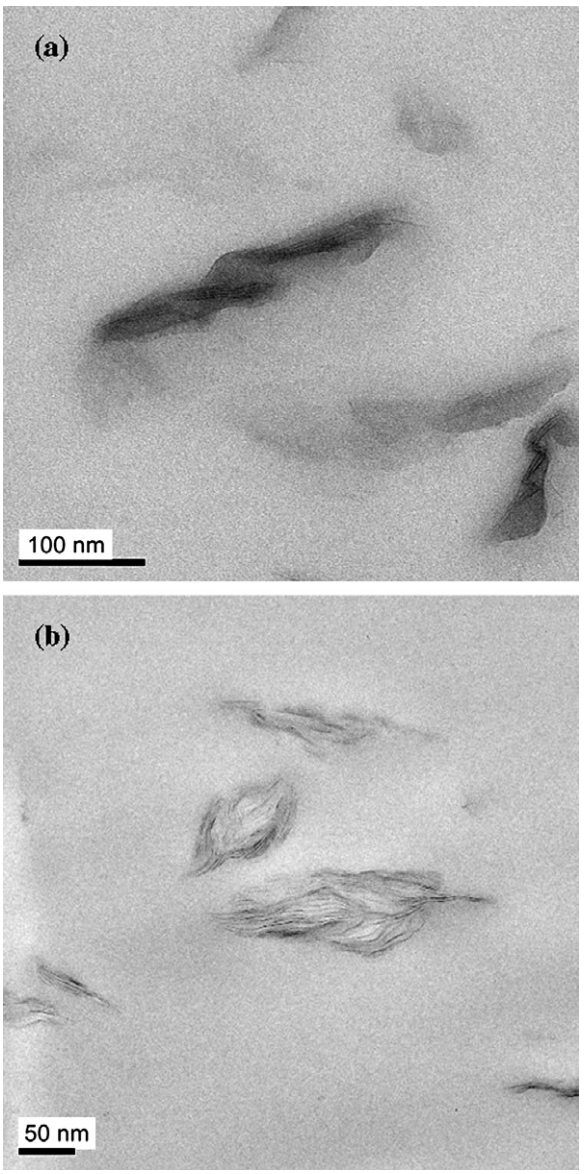

Fig. 2. TEM images of (a) PCN4 and (b) PCN44 samples.

Fig. 3 shows the dependence of unitary normalized dynamic storage modulus on the strain (γ_0) for PCNs with various epoxy contents. The linear region increases somewhat with increasing of epoxy contents. This also confirms that the compatibility between PC matrix and clay is improved due to the addition of epoxy. Thus there are more PC chains randomly tangled around the clay tactoids than that of sample without epoxy, leading to extension of the linear viscoelastic region. After critical strain values the curves all drop down, showing shear thinning behavior, a typical feature of entangled polymeric materials. Accordingly, the following SAOS measurements were conducted at $\gamma_0 = 1\%$.

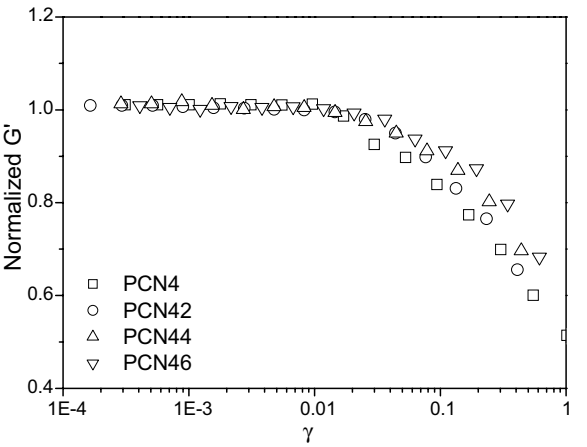

Fig. 3. The normalized storage modulus for the PCNs samples (a) without epoxy and (b) with epoxy in dynamic strain sweep.

The storage modulus (G') obtained from dynamic frequency scan measurements for PCNs samples are showed in Fig. 4. Clearly, the G' increases monotonously with increasing of epoxy loadings at low-frequency region. Li et al. [27] considered that the contribution of intercalated clay to G' of the nanocomposites (G'_{nano}) could be analyzed in terms of two effects: the confinement effect (G'_{con}) and the inter-particle interactions (G'_{inter}), which result in enhancement of low-frequency G' in comparison with the polymer matrix (G'_{matrix}), i.e.,

$$G'_{nano} = G'_{matrix} + G'_{con} + G'_{inter} \quad (1)$$

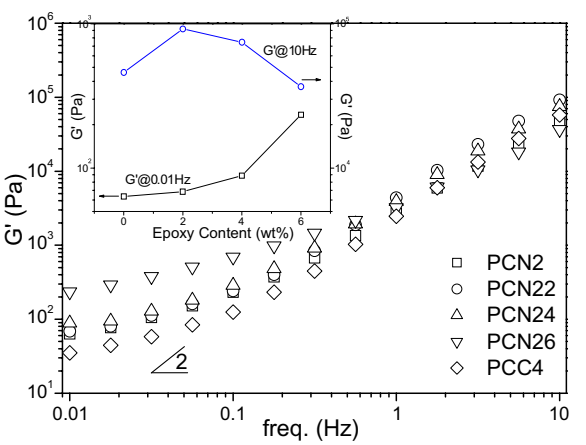

Fig. 4. The dynamic storage modulus for the PCN2s samples with various epoxy loadings.

here G'_{con} arises from the confinement of silicate layers with an interlayer distance smaller than or of the same order of the size of the chain coils that may lead to the alternation of the relaxing dynamic of the intercalated polymers, and G'_{inter} comes from frictional interactions among the tactoids, which is dominant role on the low-frequency solid-like response of PLSNs. For PCNs in this work, considering small addition of the third component, epoxy, as a compatibilizer, a term G'_{com} that arises from the presence of interface and/or interfacial interaction between the matrix and compatibilizer can be introduced in the formula (1):

$$G'_{nano} = G'_{matrix} + G'_{con} + G'_{inter} + G'_{com} \quad (2)$$

With the addition of epoxy, on the one hand, the enhanced detachment level of clay leads to formation of much more tactoids, and the load transferability among them is more effective as a result. Thus, the contribution of G'_{inter} in PCNs increases and the low-frequency G' enhances sharply due to physical jamming among the tactoids themselves. On the other hand, it can be observed that low-frequency G' of the blank sample without clay, PCC4, also shows a significant deviation from classic Cox-Merz rule, indicating that the interfacial interaction between PC and epoxy has contribution to the enhancement of modulus, too. However, the low-frequency G' of PCC4 is far smaller than that of PCNs. This indicates that the low-frequency G'_{nano} may be dominated by G'_{inter} but not G'_{com}, especially in the case of high epoxy loadings.

The effect of epoxy loadings on dynamic rheological responses can be observed clearly on the inset graph in Fig. 4, which gives the dynamic storage modulus at 0.01 and 10 Hz as a function of epoxy loadings. The enhanced $G'_{0.01\ Hz}$ is mainly attributable to the improved nanoscaled structure of clay tactoids, indicating that increasing of epoxy loadings is propitious to the nice dispersion of clay. But it is also noteworthy that with increasing of epoxy loadings, $G'_{10\,Hz}$ decreases and, as epoxy contents achieving up to 6 wt%, the modulus of PCN26 is even smaller than that of PCN2. This can be attributed to at least two factors: the plasticizing effect of excessive epoxy [25] and the thermal degradation of PC matrix [6,7].

It is well known that the presence of acidic or basic impurities will enhance depolymerization of carbonic ester in PC [40]. Organoclay can produce Lewis or Bronsted acid sites in the aluminosilicate when heated over 200 °C [41,42], which as a result has an enhanced effect on the thermal degradation of PC [15,39]. Fig. 5 shows the appearance of those prepared sheet samples. The most severe color can be observed on PCN44 samples. Yoon and Paul have studied in detailed the effects of organoclay structure on color formation during melt processing [7]. They find that color formation in the PC nanocomposites depends on both the type of organoclay and the type of pristine clay employed. A surfactant containing hydroxyethyl groups and hydrocarbon tail derived from tallow generally leads to colored materials because those groups and unit promote degradation of PC matrix. Moreover, greater dispersion of the clay also leads to higher reduction in molecular weight of PC due to the increased surface area of clay exposed. On Fig. 5, it can be observed that PCN44 sample is more darkly than PCN4, while the blank sample, PCC4, shows the same achromatous and translucent appearance with neat PC. Therefore, the addition of epoxy may not lead to degradation of PC matrix directly, while can facilitate this process in the presence of organoclay, which is confirmed by the following TGA measurements.

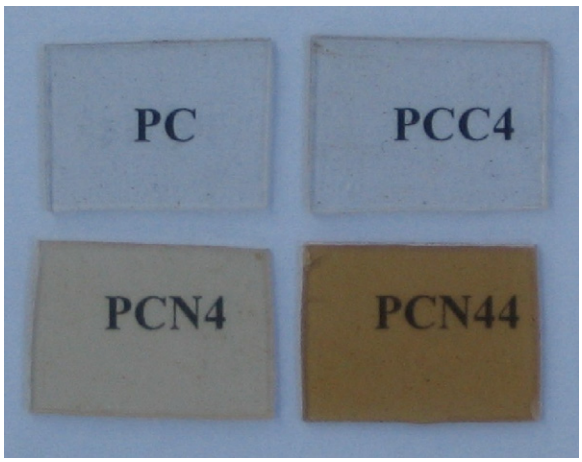

Fig. 5. The appearance of sheet samples of neat PC, PCC4, PCN4 and PCN44.

Fig. 6a gives the TGA curves for PCNs samples with various epoxy loadings. With addition of epoxy, the initial weight loss temperature decreases. However, it can be observed from enlarged region plotted in the inset graph, that PCN22 and PCN24 show higher weight loss temperature than that of PCN4 as the relative weight loss achieving up to about 5–8%. The DTG curves showed in Fig. 6b can give more detailed information. For PCN4

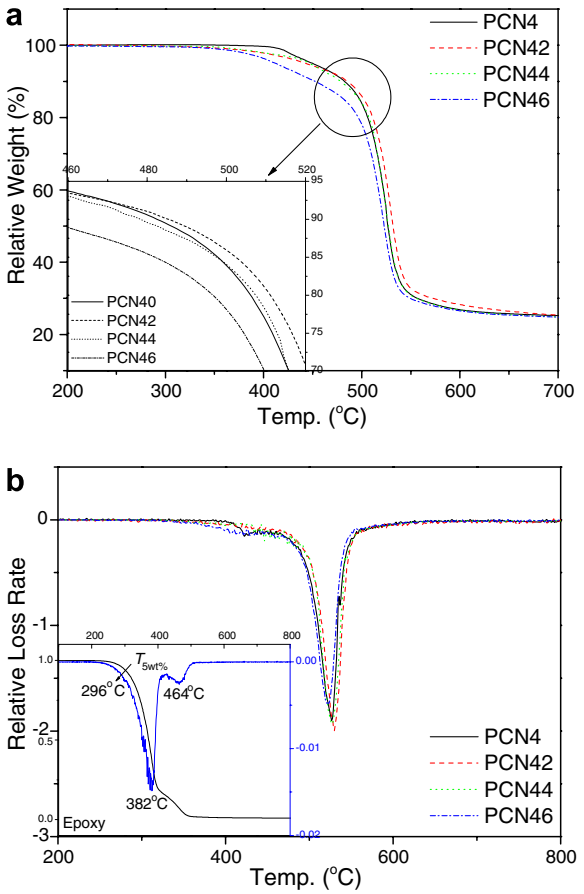

Fig. 6. (a) TG curves and (b) DTG curves for the PCN4s samples with various epoxy loadings.

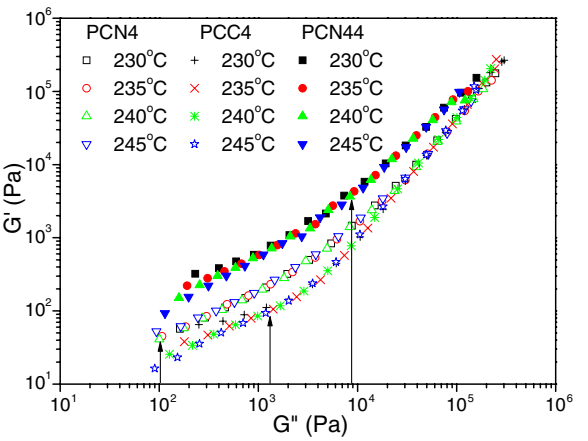

Fig. 7. Han plots of G' versus G'' for PCN4, PCN44 and PCC4 samples.

sample, the first peak comes from decomposition of the surfactant. With addition of epoxy, it becomes obtuse because of the degradation of epoxy and possible interactions between epoxy and surfactant as well as increased surface area of clay exposed. But the enhanced detachment level of tactoids creates much more physical protective barrier to retard volatilization to some extent, leading to delay of maximum decomposition rate for PCN42 and PCN44 samples. As for PCN46 sample, the worst thermal stability is due to its highest epoxy loadings. Apparently, there are many factors influencing on the thermal stability of PCNs due to the addition of the third component of epoxy. Thus the degradation mechanism of PC is complicated and is not discussed here. But at least one point can be affirmed that some kind of synergistic effect may exist between epoxy and surfactant, inducing the degradation of PC.

Therefore, it can be concluded that addition of epoxy can improve the dispersion of clay, while high loadings of epoxy lead to a severe degradation of PC matrix. To further explore the effect of epoxy on the viscoelastic properties of nanocomposites, Han plots of G' versus G'' obtained in the SAOS measurement at various temperatures are shown in Fig. 7. It is obvious that all curves deviate from the slope of 2 in low-frequency region due to the enhanced elastic responses of composites system. Han [43] believed that the rule, temperature independence of $G' \sim G''$ for homogeneous polymer systems, could be also applied to the filled polymer composites. As can be seen in Fig. 7, PCN4 sample presents temperature independence on the whole except a short region in low-frequency region. Generally, addition of clay brings two effects onto composite system: one is the interfacial adsorption between tactoids and polymer chain; the other is interaction among the tactoids themselves. Thus the temperature independence indicates that the interfacial adsorption is not the major factor influencing the viscoelastic behaviour of PCN4 and, at least in the narrow linear region, the relaxation of interaction among the tactoids is not sensitive to the experimental condition. However, with addition of epoxy, this temperature independence can not be observed on PCN44 sample. The divergence of these viscoelastic relaxations of various temperatures especially at low frequencies is mainly attributed to two factors: interfacial interactions between PC and epoxy (also confirmed by the divergence of data at low frequencies for the blank PCC4 sample) and the enhanced interfacial interactions between tactoids and PC due to the bridge role acted by the compatibilizer, epoxy (confirmed by the high-fre-

quency shift of divergence region, see the arrows in Fig. 7).

Fig. 8a and b shows the master curves superposed using frequency shift factor for PCN4 and PCN44 samples, respectively. Good superposition at high frequencies for both of these two samples is due to the dominant local chain dynamics. As expected, the principle of time–temperature superposition (TTS) fails with the rheological data at low frequencies for PCN44 in contrast to PCN4 sample. The influence of epoxy on the linear rheological behavior is evident. For horizontal shift factor, α_T, its dependence of temperature is as follows:

$$\log \alpha_T = \frac{\Delta H}{R}\left(\frac{1}{T} - \frac{1}{T_s}\right) \tag{3}$$

where ΔH is the relaxation activation energy, R is the gas constant, T_s is the reference temperature, and T, the experimental temperature. Fig. 8c gives the plots of $\log \alpha_T$ as a function of $1/T$ for PCN4 and PCN44 samples. Those plots can give quantitative ΔH as a slope providing TTS is valid. Although the principle of TTS fails with the low-frequency data of PCN4s in the presence of epoxy, the

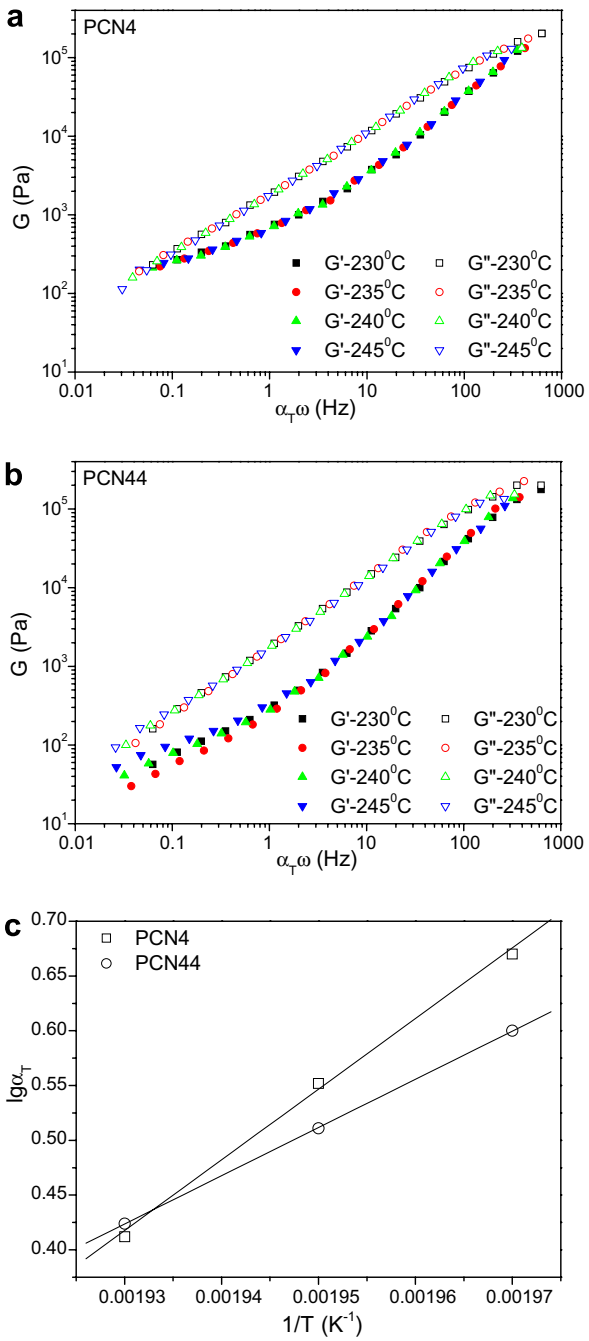

Fig. 8. Master curves of dynamic modulus versus frequency for (a) PCN4 and (b) PCN44 samples; (c) dependence of shift factors (α_T) on temperature for PCN4 and PCN44 samples.

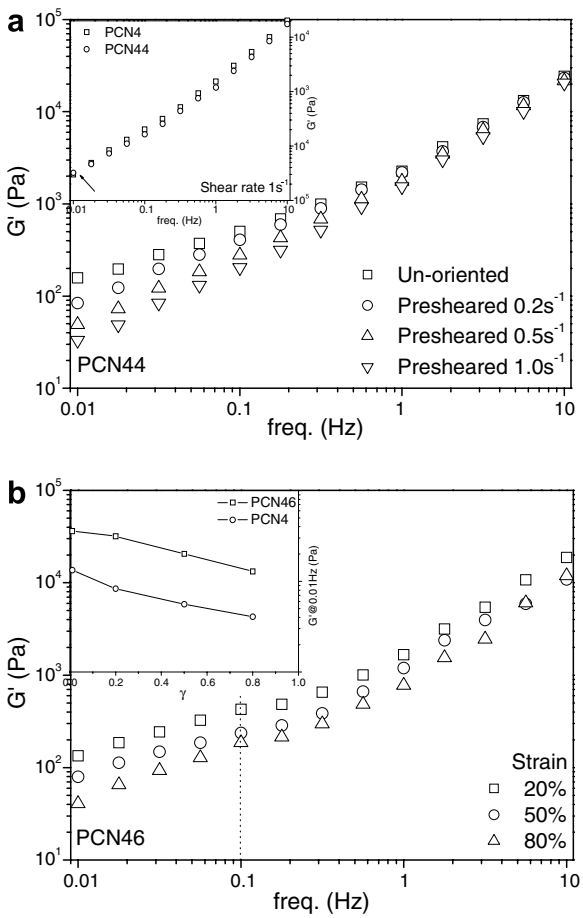

Fig. 9. Comparison of dynamic storage modulus for (a) PCN44 sample before and after preshear deformation obtained from SAOS and for (b) PCN46 sample obtained from LAOS measurements at various strains.

qualitative comparison of slope between those two samples can also give useful information. Clearly, PCN44 shows smaller slope than that of PCN4, suggesting a lower relaxation activation energy. It further confirms higher molecular weight degradation level of PC matrix with addition of epoxy.

3.3. Nonlinear dynamic rheological properties

Since linear region is very sensitive to the presence of clay, the study on linear viscoelastic properties of PCNs is limited in a quite narrow strain or stress region. The nonlinear rheological measurements, however, may facilitate further insight into mesoscopic structure of PCNs. It is believed that the percolated tactoids network formed in SAOS is very sensitive to quiescent shear flow [24,27]. Fig. 9a shows the effect of quiescent shear on SAOS responses of PCN44. The dynamic modulus of presheared PCN44 decreases with increasing of shear rates, especially at low frequencies. It suggests that the platelet-like tactoids are oriented in the shear direction and can not form a percolation network structure. As a result, the low-frequency viscoelastic responses changes from solid-like to a liquid one after quiescent preshear. Moreover, it can be observed from the inset graph in Fig. 9a that PCN44 still shows higher low-frequency modulus (see the arrow) and lower high-frequency modulus than that of PCN4 after being presheared at identical rate. This again indicates higher detachment level of clay and also higher degradation level of matrix in PCN44 in contrast to that of PCN4, which are both due to the addition of epoxy.

Fig. 9b gives dynamic modules of PCN46 obtained from LAOS measurements. Also, G' reduces remarkably with increasing of strain, indicating that the interactions among tactoids or their transient physical gelation level decreases under large shear deformation. But on the inset graph, it can be observed that PCN46 shows somewhat low sensitivity to LAOS compared to that of PCN4, especially at low strain level. This is mainly arisen from the increased percolation density and/or enhanced interactions between matrix and clay tactoids due to compatibilization of epoxy. Moreover, it is interesting that all curves in LAOS present the second plateau at the frequency of 0.1 Hz (see the dashed), which indicates a possible phase separation in matrix of PCN46 sample because that plateau is usually believed as a viscoelastic behavior corresponding to the interface and shape relaxation of dispersed domain in the immiscible polymer blend [44,45]. The SEM images showed in Fig. 10 further confirm the occurrence of phase separation. Clearly, the fractured surface of PCN46 shows numerous lacunule about not more than 1 μm in diameter, which cannot be observed on neat PC, PCCs, PCNs

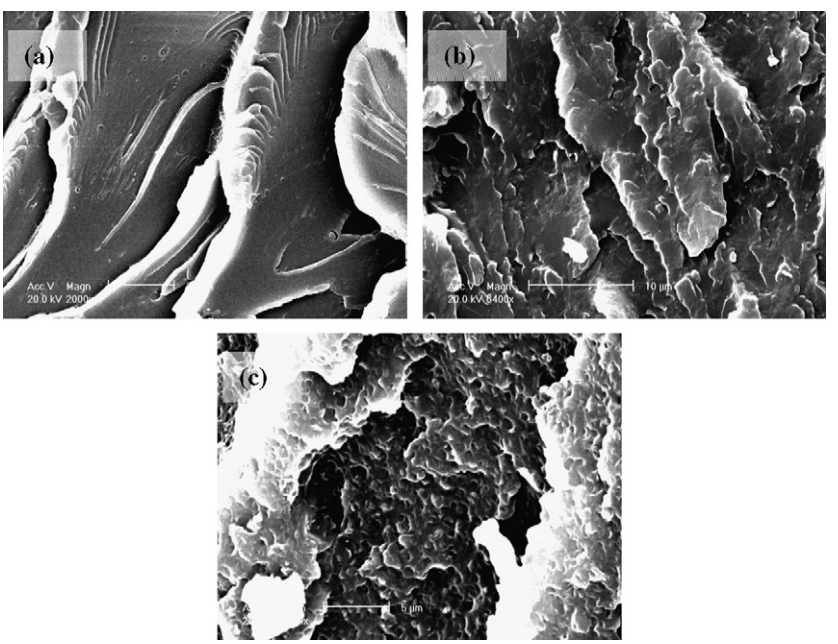

Fig. 10. SEM images of the fractured surface of (a) neat PC, (b) PCN4 and (c) PCN46 samples.

without epoxy and even on those PCNs with low epoxy loadings (<4 wt%). This is a typical reaction induced phase separation (RIPS) during the depolymerization process [46–48]. Both the degradation and RIPS mechanism especially under shear deformation will be reported soon in another paper.

4. Conclusions

In this study, intercalated PCNs were prepared via melt mixing using epoxy as a compatibilizer. The effect of epoxy on the rheology of nanocomposites was studied detailedly. Addition of epoxy not only results in increasing of detachment level of clay tactoids, but also leads to a severe degradation of PC matrix due to the synergistic effect with surfactant, both influencing the dynamic rheological behaviour remarkably. The percolation network of clay tactoids is easily ruptured by both the quiescent and the large amplitude oscillatory shear deformation despite addition of epoxy. The presence of epoxy has no evident influence on the relaxation behavior of network in the experimental scale but can reduce relaxation activation energy of PC matrix.

Acknowledgements

This work was supported by the research grants from the National Natural Science Foundation of China (No. 50373034) and Foundation of Jiangsu Provincial Key Program of Physical Chemistry in Yangzhou University.

References

[1] Usuki A, Hasegawa N, Kato M. Polymer–clay nanocomposites. Adv Polym Sci 2005;179:135–95.
[2] Ray SS, Kato M. Polymer/layered silicate nanocomposites: a review from preparation to processing. Prog Polym Sci 2003;28:1539–641.
[3] Alexandre M, Dubois P. Polymer-layered silicate nanocomposites: preparation, properties and uses of a new class of materials. Mater Sci Eng 2000;28:1–63.
[4] LeGrand DG, Bendler JT. Handbook of polycarbonate science and technology. New York: Marcel Dekker; 2000.
[5] Yoon PJ, Hunter DL, Paul DR. Polycarbonate nanocomposites. Part 1. Effect of organoclay structure on morphology and properties. Polymer 2003;44:5323–39.
[6] Yoon PJ, Hunter DL, Paul DR. Polycarbonate nanocomposites: Part 2. Degradation and color formation. Polymer 2003;44:5341–54.
[7] Hsieh AJ, Moy P, Beyer FL, Madison P, Napadensky E, Ren JX, et al. Mechanical response and rheological properties of polycarbonate layered-silicate nanocomposites. Polym Eng Sci 2004;44:825–31.
[8] Lee KM, Han CD. Effect of hydrogen bonding on the rheology of polycarbonate/organoclay nanocomposites. Polymer 2003;44:4573–88.
[9] Yoo YJ, Choi KY, Lee JH. Polycarbonate/montmorillonite nanocomposites prepared by microwave-aided solid state polymerization. Macromol Chem Phys 2004;205:1863–8.
[10] Hu XB, Lesser AJ. Enhanced crystallization of bisphenol-a polycarbonate by nano-scale clays in the presence of supercritical carbon dioxide. Polymer 2004;45:2333–40.
[11] Mitsunaga M, Ito Y, Ray SS, Okamoto M, Hironaka K. Intercalated polycarbonate/clay nanocomposites: nanostructure control and foam processing. Macromol Mater Eng 2003;288:543–8.
[12] Ito Y, Yamashita MS, Okamoto M. Foam processing and cellular structure of polycarbonate-based nanocomposites. Macromol Mater Eng 2006;291:773–83.
[13] Ray SS, Bousmina M. Morphology and properties of organoclay modified polycarbonate/poly(methyl methacrylate) blend. Polym Eng Sci 2006;46:1121–9.
[14] Zong RW, Hua Y, Wang SF, Song L. Thermogravimetric evaluation of PC/ABS/montmorillonite nanocomposites. Polym Degrad Stab 2004;83:423–8.
[15] Wang SF, Hu Y, Song L, Liu J, Chen ZY, Fan WC. Study on the dynamic self-organization of montmorillonite in two phases. J Appl Polym Sci 2004;91:1457–62.
[16] Wang SF, Hua Y, Wang ZZ, Yong T, Chen ZY, Fan WC. Synthesis and characterization of polycarbonate/ABS/montmorillonite nanocomposites. Polym Degrad Stab 2003;80:157–161.
[17] Gonzalez I, Eguiazabal JI, Nazabal J. New clay-reinforced nanocomposites based on a polycarbonate/polycaprolactone blend. Polym Eng Sci 2006;46:864–73.
[18] Krishnamoorti R, Giannelis EP. Rheology of end-tethered polymer layered silicate nanocomposites. Macromolecules 1997;30:4097–102.
[19] Krishnamoorti R, Vaia RA, Giannelis EP. Structure and dynamics of polymer-layered silicate nanocomposites. Chem. Mater. 1996;8:1728–34.
[20] Ren J, Silva AS, Krishnamoorti R. Linear viscosity of disordered polystyrene–polyisoprene block copolymer based layered-silicate nanocomposites. Macromolecules 2000;33:3739–3746.
[21] Galgali G, Ramesh C, Lele A. A rheological study on the kinetics of hybrid formation in polypropylene nanocomposites. Macromolecules 2001;34:852–8.
[22] Lim YT, Par OO. Phase morphology and rheological behavior of polymer clay nanocomposites. Rheol Acta 2001;40:220–9.
[23] Solomon MJ, Almusallam AS, Seefeldt KF, Varadan P. Rheology of polypropylene/clay hybrid materials. Macromolecules 2001;34:1864–72.
[24] Wu DF, Zhou CX, Xie F, Mao DL, Zhang B. Study on rheological behavior of poly(butylene terephthalate)/montmorillonite nanocomposites. Eur Polym J 2005;41:2199–207.
[25] Wu DF, Zhou CX, Yu W, Xie F. Effect of flocculated structure on rheology of poly(butylene terephthalate)/clay nanocomposites. J Polym Sci Part B Polym Phys 2005;43:2807–2818.
[26] Wan T, Clifford MJ, Gao F, Bailey AS, Gregory DH, Somsunan R. Strain amplitude response and the microstructure of PA/clay nanocomposites. Polymer 2005;46:6429–6436.

[27] Li J, Zhou CX, Wang G. Study on rheological behavior of polypropylene/clay nanocomposites. J Appl Polym Sci 2003; 89:3609–16.
[28] Okamoto M, Taguchi H, Sato H, Kotaka T, Tateyama H. Dispersed structure and rheology of lipophilized-smectite/ toluene suspensions. Langmuir 2000;16:4055–8.
[29] Wu DF, Wu L, Wu LF, Zhang M. Rheology and thermal stability of polylactide/clay nanocomposites. Polym Degrad Stab 2006;91:3149–55.
[30] Ray SS, Bousmina M. Effect of organic modification on the compatibilization efficiency of clay in an immiscible polymer blend. Macromol Rapid Commun 2005;26:1639–46.
[31] Becker O, Simon GP. Epoxy layered silicate nanocomposites. Adv Polym Sci 2005;179:29–82.
[32] Peng M, Li HB, Wu LJ, Chen Y, Zheng Q, Gu WF. Organically modified layered-silicates facilitate the formation of interconnected structure in the reaction-induced phase separation of epoxy/thermoplastic hybrid nanocomposite. Polymer 2005;46:7612–23.
[33] Liu XH, Wu QJ, Berglund LA. Polymorphism in polyamide 66/clay nanocomposites. Polymer 2002;43:4967–72.
[34] Liu XH, Wu QJ, Berglund LA, Lindberg H, Fan JQ, Qi ZN. Polyamide 6/clay nanocomposites using a cointercalation organophilic clay via melt compounding. J Appl Polym Sci 2003;88:953–8.
[35] Park JH, Jana SC. The relationship between nano- and micro-structures and mechanical properties in PMMA–epoxy–nanoclay composites. Polymer 2003;44:2091–100.
[36] Isik I, Yilmazer U, Bayram G. Impact modified epoxy/ montmorillonite nanocomposites: synthesis and characterization. Polymer 2003;44:6371–7.
[37] Frohlich J, Thomann R, Gryshchuk O, Karger-Kocsis J, Mulhaupt R. High-performance epoxy hybrid nanocomposites containing organophilic layered silicates and compatibilized liquid rubber. J Appl Polym Sci 2004;92:3088–96.
[38] Guo BC, Jia DM, Cai CG. Effects of organo-montmorillonite dispersion on thermal stability of epoxy resin nanocomposites. Eur Polym J 2004;40:1743–8.
[39] Gao X, Mao LX, Jin RG, Zhang LQ, Tian M. Preparation and characterization of polycarbonate/polypropylene/ attapulgite ternary nanocomposites with the morphology of encapsulation. Macromol Mater Eng 2005;290:899–905.
[40] Gachter R, Muller H. Plastics additives. 4th ed. Munich: Hanser Publishers; 1993.
[41] Xie W, Gao Z, Pan WP, Hunter D, Singh A, Vaia R. Thermal degradation chemistry of alkyl quaternary ammonium montmorillonite. Chem Mater 2001;13:2979–90.
[42] Zanetti M, Camino G, Canavese D, Morgan AB, Lamelas FL, Wilkie CA. Fire retardant halogen–antimony–clay synergism in polypropylene layered silicate nanocomposites. Chem Mater 2002;14:189–93.
[43] Han CD, Kim JK. On the use of time–temperature superposition in multicomponent/multiphase polymer systems. Polymer 1993;34:2533–9.
[44] Utracki LA. Polymer blends & alloys: thermodynamics & rheology. New York: Hanser Publishers; 1989.
[45] Utracki LA, Kamal MR. Melt rheology of polymer blends. Polym Eng Sci 1982;22:96–105.
[46] Park SJ, Seo DI, Lee JR. Surface modification of montmorillonite on surface acid–base characteristics of clay and thermal stability of epoxy/clay nanocomposites. J Colloid Interface Sci 2002;251:160–5.
[47] Uyar T, Tonelli AE, Hacaloglu J. Thermal degradation of polycarbonate, poly(vinyl acetate) and their blends. Polym Degrad Stab 2006;91:2960–7.
[48] Poel GV, Goossens S, Goderis B, Groeninckx G. Reaction induced phase separation in semicrystalline thermoplastic/ epoxy resin blends. Polymer 2005;46:10758–71.